

Acoustic properties of Neogene carbonates and siliciclastics from the subsurface of the Florida Keys: implications for seismic reflectivity

Flavio S. Anselmetti¹*, Gian A. von Salis², Kevin J. Cunningham, Gregor P. Eberli

Comparative Sedimentology Laboratory, RSMAS/MGG, University of Miami, 4600 Rickenbacker Causeway, Miami, FL 33149, USA

Received 14 January 1997; received in revised form 30 June 1997; accepted 30 June 1997

Abstract

Results of measurements of compressional-wave velocity and shear-wave velocity have been compared with other rock properties, XRD and thin-section analyses for over fifty minicores from two cores drilled through sedimentary rocks on Stock Island and Long Key (Florida Keys). The comparisons indicate that sonic velocity in siliciclastics and carbonates is mainly controlled by three factors: (1) porosity and primary pore type, (2) quartz content and (3) dolomite content. In the case of two Pliocene prograding formations, the combination of depositional fabric and diagenetic alterations produced patterns and values of almost identical impedance for fine-grained carbonates and siliciclastics. Consequently, seismic sections can not be used to distinguish between the prograding quartz sands and the prograding fine-grained carbonates. Compressional and shear-wave velocities in the limestones are strongly controlled by total porosity and the primary pore type. Generally, high-porosity rocks have lower velocities than low-porosity rocks, but pore types can significantly influence velocities. Overall, an increasing percentage of dolomite in carbonate rocks results in an increase in velocity. Some dolomitic fabrics deviate from this trend. Fabric preserving, mimetic dolomites yield the highest velocities, whereas samples that are of purely sucrosic dolomites produce lower velocities, which, however, are still higher in average than non- or only partly dolomitized samples. Quartz sandstones and quartz-bearing limestones have generally low and uniform velocities. The low velocities of the sandstones containing >80% quartz is a result of their primary interparticle porosity. Due to the low diagenetic potential of quartz grains, a high quartz content inhibits major diagenetic alterations, which would result in cementation and higher velocities. Synthetic seismograms and nearby seismic sections reveal two major seismic facies as a result of the observed velocity distribution: (1) carbonates of the Stock Island Formation and siliciclastics of the Long Key Formation are both characterized by low seismic reflectivity or even seismic transparency. This seismic facies is caused by a very similar, uniform, vertical distribution of low velocities with almost identical impedance values in the two formations. Thus, the transition or an interfingering between the time-equivalent siliciclastic Long Key Formation and the carbonate Stock Island Formation might not be detectable on a seismic section. (2) The over- and underlying shallow-marine carbonates, in contrast, have higher velocities with a wider range of velocities resulting in a succession of high-amplitude reflections. © 1997 Elsevier Science B.V.

Keywords: physical properties; sound velocity; carbonates; siliciclastics; seismic facies; seismic modeling

* Corresponding author. Tel.: +41 41 1 632 6569; fax.: +41 41 1 632 1080; e-mail: flavio@erdw.ethz.ch

¹ Current address: Institute of Geology, Swiss Federal Institute of Technology, ETH, 8092 Zürich, Switzerland.

² Current address: Institute of Geophysics, Swiss Federal Institute of Technology, ETH, 8093 Zürich, Switzerland.

1. Introduction

This study focuses on measurements of physical properties of two cores, which are part of the Florida Keys Drilling Project (Cunningham et al., 1995, 1997; Ginsburg and Cunningham, 1996; Warzeski et al., 1996). This study presents results and interpretations of laboratory measurements on core data, wire-line logging data and seismic data, and thus integrates lithology, physical properties, and seismic response of the sedimentary rocks in the Florida Keys subsurface. The Florida Keys Drilling Project is investigating the stratigraphic architecture of the subsurface of the Florida Keys. In 1994, a seismic survey was conducted from Rice University's R/V *Lone Star* using a 15 cu. in. SSI Watergun (Warzeski et al., 1996). Several dip lines across the outer shelf and shallow slope were positioned to tie the nearby wells. Strike lines connecting the dip-oriented profiles were positioned along the shallow slope seaward of the southern Florida Shelf margin to maximize penetration and to minimize interference from multiples. The seismic data were processed at the University of Miami Seismic Laboratory. Shallow water prevented the continuation of the seismic survey from intersecting the drillsites on the islands. However, the cores from the wells located on the Keys represent the closest lithologic database providing insight into the lithologic parameters affecting the observed seismic reflection patterns.

One goal of this study was to investigate the controls and variability of sonic velocity in the carbonate and the mixed carbonate siliciclastic strata, and to relate this to the nearby seismic images. Studies of the controls and variations of sonic velocities have often concentrated on either siliciclastic rocks (e.g. Han et al., 1986; Marion et al., 1992; Vernik and Nur, 1992; Vernik, 1994) or on pure carbonates (e.g. Rafavich et al., 1984; Wang et al., 1991; Anselmetti and Eberli, 1993). The few existing studies of velocity distribution in mixed carbonate–siliciclastic sediments, however, are mainly limited to highly altered Paleozoic sediments (Christensen and Szymanski, 1991; Kenter et al., 1997). The cores of the Neogene-to-Quaternary mixtures of siliciclastic and carbonate

sediments of the Florida Keys offer thus an unique opportunity to investigate the signatures of petrophysical properties in mixed sediments of younger age and to correlate them to nearby shallow-marine seismic data.

In addition, available sonic and density wire-line logs allow for modeling of the seismic response through computation of synthetic seismograms. The seismograms of the core holes are compared with the seismic reflection pattern from the off-shore seismic lines. They help explain the inherent reflectivity of the different lithologies and the character of the seismic pattern.

2. Methods

Two nearly continuous cores are used in this study, both drilled by the Florida Geological Survey. The core holes are located in the Florida Keys on Stock Island and Long Key (Fig. 1). The Stock Island core hole was cored to a depth of 325.5 m and the Long Key core hole to 427.0 m. Thirty-four miniplugs from the Long Key core and twenty miniplugs from the Stock Island core were taken representing all major lithologies. The cylindrical minicores are 14 to 32 mm long and are 2.52 cm (1 inch) in diameter. The following analyses were performed.

Prior to velocity measurements, the ends of the plugs were polished and all samples were oven-dried and weighed. Dry density was calculated by dividing the weight by its bulk volume, obtained by measuring length and diameter. The samples were powdered to eliminate any closed porosity, then dried for 48 h at ~60°C and stored in a desiccator. Grain density was determined with a helium pycnometer. The difference between dry bulk density and grain density determines the porosity of the sample through the following formula:

$$\text{Porosity (\%)} = \frac{\rho_{\text{grain}} - \rho_{\text{dry}}}{\rho_{\text{grain}}} \times 100$$

(ρ_{grain} = grain density;

ρ_{dry} = dry density of dried plug)

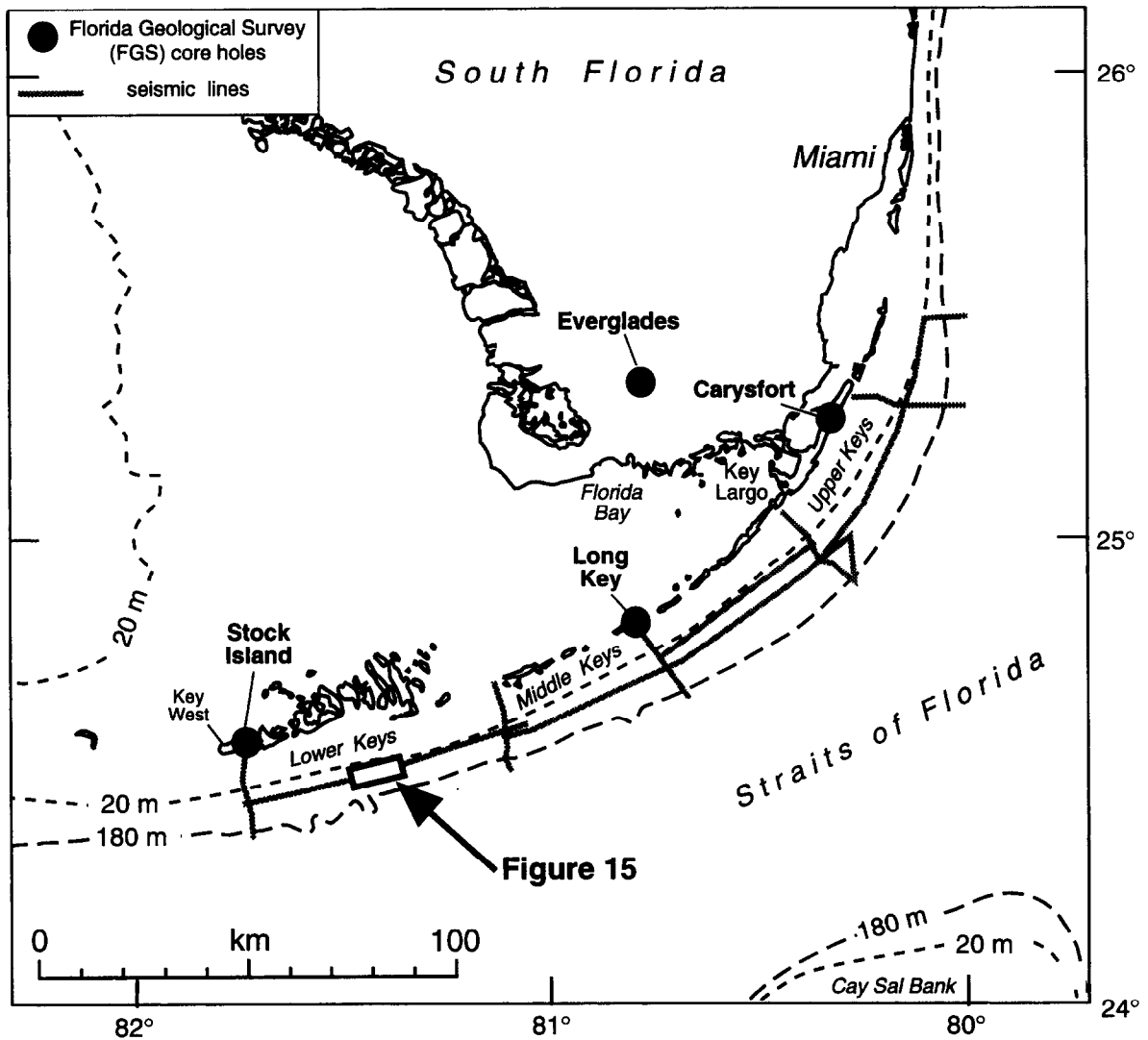


Fig. 1. Map of South Florida with location of core holes drilled by the Florida Geological Survey. The cores at Stock Island and Long Key were used in this study. The locations of the marine seismic sections are displayed in thick gray lines.

Unlike other methods that are based on penetration of a fluid into the pore space (Archimedes method, dry versus saturated weight method), our value includes isolated porosity and, thus, represents total porosity, because grain density was determined on the powdered samples.

Ultrasonic velocities of all minicores were measured with a pair of piezoelectric transducers that create one ultrasonic compressional wave (V_p) and two perpendicular polarized shear-wave signals (V_s) with a frequency of 0.6–1.2 MHz (Birch,

1960). Confining and pore fluid pressures were selected independently, allowing for an accurate simulation of burial conditions of the rocks. The sample was lined with a flexible jacket to seal the confining oil from the pore fluid system within the minicore. Pore fluid pressure was held constant at 2 MPa, while the confining pressure was varied between 5 and 80 MPa. This resulted in an effective pressure (the difference between confining pressure and pore fluid pressure) between 3 and 78 MPa.

The percentages of the amounts of quartz, ara-

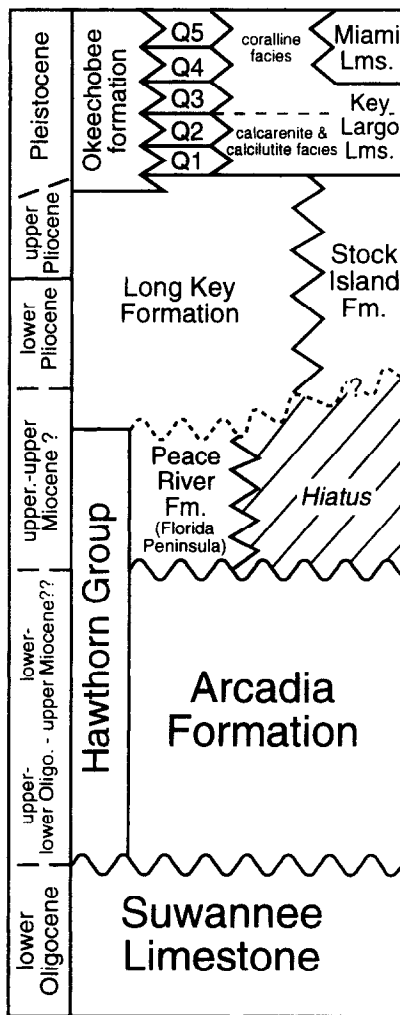


Fig. 2. Stratigraphic column for the late Cenozoic of southernmost Florida (from Cunningham et al., 1997).

gonite, low-magnesium calcite, high-magnesium calcite and dolomite were calculated from peak-area ratios produced by a Scintag XDS-2000 X-ray diffraction unit.

Thin-section samples from miniplugs enabled us to investigate parameters such as pore size, pore types, depositional textures, lithology and diagenetic alterations. Depositional textures were classified according to Dunham (1962). If dolomite was present, the dolomite was classified into fabric-preserving mimetic or sucrosic dolomite (Dawans and Swart, 1988). The non-carbonate samples

were mostly fine-grained, pure quartz sands with relatively little clay content.

In addition to these laboratory measurements, a suite of wire-line logs was available for both core holes. Sonic logs and density logs are displayed as continuous downhole measurements and show vertical trends with higher resolution than discrete samples. These logs were also used to compute synthetic seismograms for both core holes, which simulates the seismic response of the drilled sections. Seismograms were calculated at the reflection seismology laboratory of the Swiss Federal Institute of Technology ETH, Zürich. Finally, the petrophysical signatures and the synthetic seismograms were compared with seismic data from further offshore.

3. Regional geology and lithology of the cores

The Florida Keys are an archipelago of islands that separate the deep-water Atlantic (Florida Straits) from the shallow-water Florida Bay (Fig. 1). The position of the Florida Keys mimics a topographic high created by a Pleistocene barrier reef, mainly made of Key Largo limestone, a reefal limestone, which forms a relief over Upper Pleistocene fore- and backreef sediments. High-resolution seismic surveys west of the Florida Keys at the southern end of the Florida Platform indicate several southward prograding slope sequences deposited in the late Quaternary (Brooks and Holmes, 1989; Locker and Hine, 1995). Although Florida is a modern carbonate province, these Quaternary carbonates rest on upper Tertiary siliciclastics (Vaughan, 1910; Matson and Sanford, 1913; Jordan et al., 1964). Ginsburg et al. (1989) suggested that a combination of longshore and riverine transport carried these siliciclastics to the southern end of the Florida Platform. Since Jordan et al. (1964), several authors have speculated that currents and waves redistributed these siliciclastics to form a giant, spit-like platform that served as a foundation for the Quaternary reefs of the Florida Keys (Ginsburg et al., 1989). In 1993, the University of Miami and Florida Geological Survey (FGS) initiated the Florida Keys Drilling Project (FKDP). The FKDP has collected fifteen

marine seismic profiles seaward of the Florida Keys, and has drilled three deep continuous core holes in the Keys (Stock Island, Long Key and Carysfort Cores; Fig. 1) and one on the southern Peninsula of Florida (Everglades Core; Fig. 1). Warzeski et al. (1996) documented with these new core holes and marine seismic profiles the distribution and paleoenvironments of the siliciclastic foundation sandwiched between the Quaternary carbonates (Key Largo Formation) and the Oligocene and Miocene carbonates (Arcadia Formation). The lithologies of the core holes, however, revealed that the 30 m thick Quaternary carbonates are underlain by both, a mixture of limestone and siliciclastics, and marine siliciclastics (Warzeski et al., 1996). Their findings resulted in the redefinition of the Neogene lithostratigraphy of South Florida (Fig. 2) (Cunningham et al., 1997), which will be summarized below.

3.1. *Arcadia Formation*

The lithologies of the Arcadia Formation are mainly lime floatstones, rudstones, grainstones, packstones and dolomites. Principle grains are skeletal fragments, mollusks, benthic foraminiferas, red algae and echinoids. Arcadia deposition occurred in the Keys on a carbonate ramp probably influenced by temperate conditions (Cunningham et al., 1997). The top of the Arcadia is bounded by a regional unconformity and subaerial exposure surface that is typically characterized by a thin layer of black phosphorite.

The range in the age of the Arcadia Formation has been reported as young as early late Miocene (Cunningham et al., 1997) and as old as early late Oligocene (Brewster-Wingard et al., 1997).

3.2. *Long Key Formation*

The Long Key Formation is a new formational name proposed by Cunningham et al. (1997) for a succession of subsurface siliciclastics up to 145 m thick underlying the Florida Keys, suprajacent to the Arcadia Formation, subjacent to the Key Largo and Miami Limestones (Fig. 2), and laterally equivalent to the Stock Island Formation (Fig. 3). The regional unconformity at the base

of the Long Key Formation forms a major temporal hiatus, at the millions of years scale (Guertin et al., in prep.). Warzeski et al. (1996) showed that marine seismic data just south of the Florida Keys suggests that downlapping beds of the Long Key Formation prograded southward to eastward over the unconformity at the top of the Arcadia Formation.

The lithology is principally a very fine to fine sand-size quartz sand or sandstone (Fig. 4b). The thickness of the Long Key Formation at the type locality is 143.7 m and occurs between core depths of 48.2 and 191.9 m. The upper contact of the Long Key Formation is gradational to abrupt with overlying quartz-sand-rich, bioclastic wackestones and packstones of the Key Largo Formation. The relationship between the Stock Island Formation and the Long Key Formation appears to be a gradual lateral change in facies. The boundary between the two formations is placed at the lateral transition between Stock Island planktic foraminiferal lime grainstones or packstones, which contain $\leq 50\%$ siliciclastic sand grains, and siliciclastic sandstones of the Long Key Formation, which contain $\leq 50\%$ planktic foraminiferal lime grainstones or packstones. In the Florida Keys, the Long Key Formation has been identified as far west as the Gulf Oil, State Lease No. 373, No. 1 well (FGS No. W-972) on Big Pine Key (Fig. 3).

Analyses of planktic foraminiferas indicate that the siliciclastics of the Long Key Formation have a maximum age of Messinian and a minimum age of Gelasian (Guertin et al., in prep.).

3.3. *Stock Island Formation*

The Stock Island Formation was proposed by Cunningham et al. (1997) as a new formational name for subsurface fine-grained limestones that are suprajacent to the Arcadia Formation, subjacent to the Key Largo Limestone, and laterally equivalent to the Long Key Formation (Fig. 3). The Stock Island Formation extends westward of the Long Key Formation between the middle and lower Keys (Fig. 3). Marine seismic data suggest that beneath the Florida Keys, beds of the Stock Island Formation prograde southward and downlap onto the regional unconformity at the

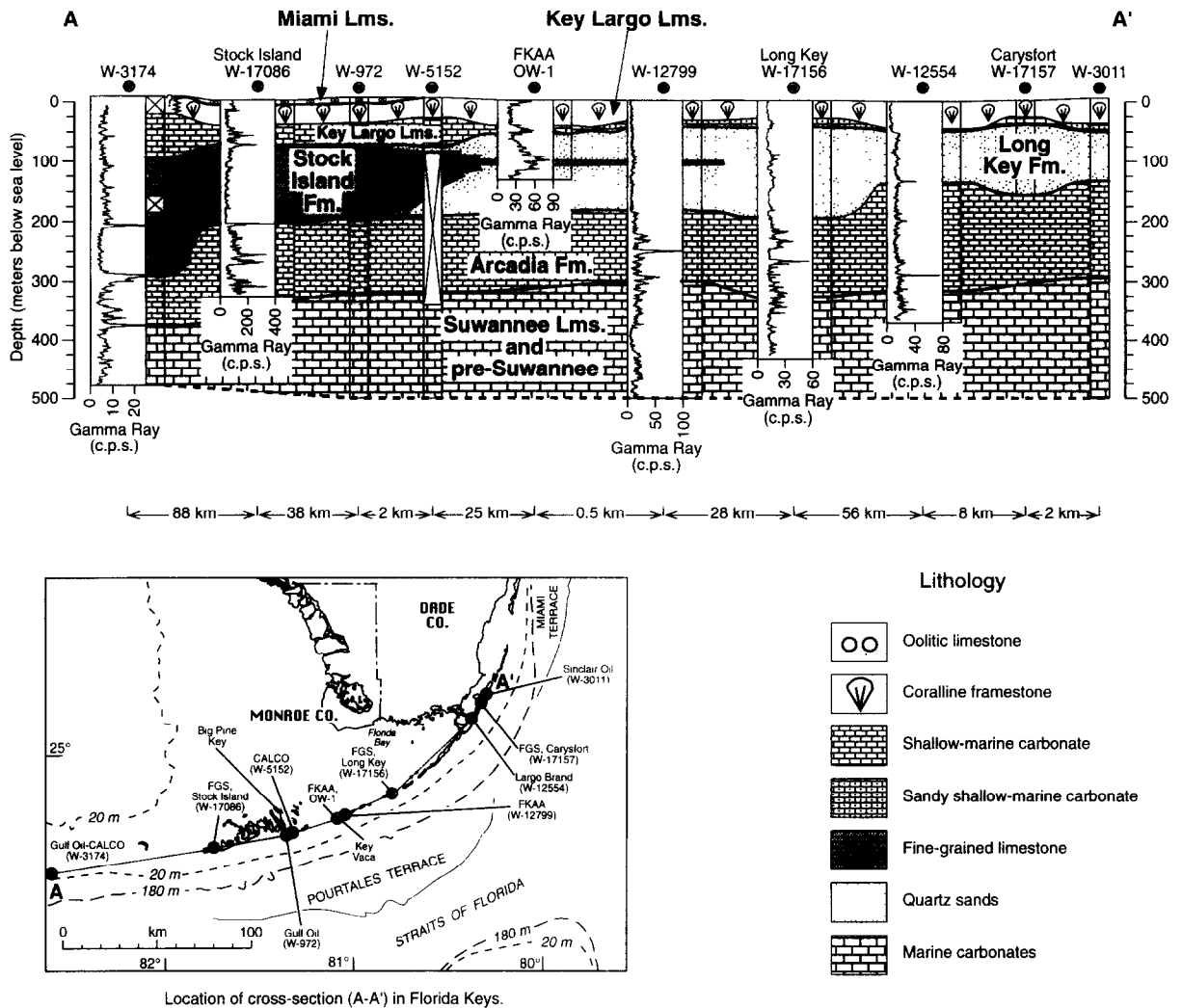


Fig. 3. Stratigraphic context of the two core holes on Long Key and Stock Island and of other core holes along a transect connecting the Florida Keys. Gamma ray log data are shown for correlation.

top of the Arcadia Formation (Warzeski et al., 1996).

The principle lithologies are moldic skeletal and planktic foraminiferal lime grainstones and well-washed lime packstones (Fig. 4a). The thickness of the Stock Island Formation at the type locality is 121.3 m and occurs between core depths of 85.5 and 206.8 m. The upper contact of the Stock Island Formation is gradational with overlying floatstones.

Results from planktic foraminiferal analyses by Guertin (personal communication) indicate that

the limestones of the Stock Island Formation have a maximum age of Zanclean and a minimum age of Piacenzian.

4. Results

4.1. Laboratory data

The following values were recorded from all samples from both the Long Key and Stock Island cores. Acoustic data were taken at a confining

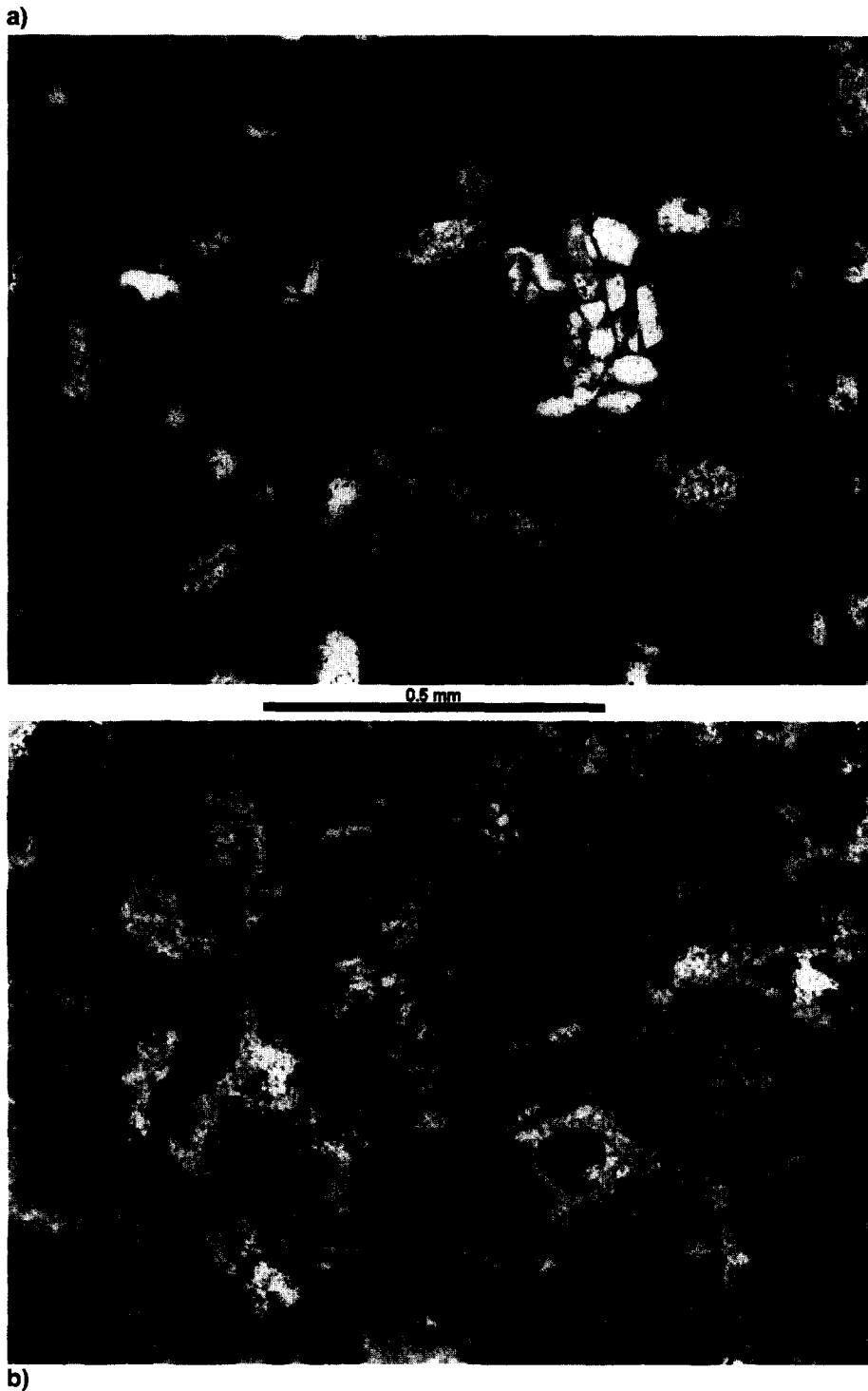


Fig. 4. Thin-section examples of the time-equivalent Stock Island and Long Key Formations. (a) Sample from Stock Island core, 182.1 m depth. Fine-grained, globigerina-rich packstone. Quartz content (white grains) is less than 5%. Porosity appears grey. (b) Sample from Long Key core, 124.7 m depth. The sediment consists almost purely of well-sorted quartz grains (appearing dark with white spots), with occasional globigerinas. Porosity appears light grey.

pressure of 10 MPa and a pore fluid pressure of 2 MPa, resulting in an effective pressure of 8 MPa. Depending on the assumed hydrostatic conditions, such a pressure is equivalent of a burial depth between 300 and 800 m. Physical properties and lithological parameters of all samples are shown in Table 1

4.1.1. V_p and V_s

V_p from the measured minicores from Long Key and Stock Island at an effective pressure of 8 MPa range from 1710 to 5965 m/s. V_s varies from 976 to 3287 m/s (Table 1). The two extreme values of V_s originate from within 9 m in the Stock Island core, documenting the strong heterogeneities in some sections of the core. The pressure dependence of the velocities is shown in Fig. 5. In general, sonic velocities increase with increasing effective pressure. Samples with a low velocity have steeper velocity gradients compared to samples with higher sonic velocities that are characterized by a minimal velocity increase at elevated pressures.

The V_p/V_s ratio varies between 1.7 and 2.4. There is a very weak correlation between the V_p/V_s ratio and the porosity (Fig. 6). In general, the ratio increases with increasing porosity and varies more in high-porosity sediments than in low-porosity sediments. V_s seems more effected by high-porous fabrics than V_p . As a result, the V_s decrease is stronger compared to V_p decrease, resulting in an increasing V_p/V_s ratio at higher porosities.

4.1.2. Acoustic impedances

Compressional wave velocities and bulk densities were used to calculate acoustic impedances. The impedance ranges from 2.5 to $15.3 \cdot 10^6$ kg · s/m² which is a remarkable 6-fold range for the late Neogene to Quaternary rocks. Since changes in impedance cause reflection of acoustic waves, such a high range explains the good reflectivity in sections with highly variable lithologies.

4.1.3. Porosity

The porosities of all samples of the two core holes range between 9 to 56%. Similar to the lack of a downhole velocity trend, porosity shows no clear downhole decrease (Table 1) as seen for

instance in deep-water pelagic sediments (Hamilton, 1980). The lack of such a trend documents that the cored rocks are strongly influenced by post-depositional, diagenetic changes in texture and pore structure. For example, the four highest total porosities were measured in samples that all have moldic secondary porosity as principal pore type, indicating the importance of diagenesis in downhole porosity evolution.

4.1.4. Mineralogy

The weight percentages of mineral components are displayed in Table 1. The samples from the Long Key core between 45 and 200 m are characterized by quartz contents of 80% and higher. Above, quartz content decreases gradually and the two shallowest samples consist of 100% low-Mg calcite. Below 200 m depth, the samples consist of a mixture of low-Mg calcite and dolomite. Most samples between 260 and 326 m are completely dolomitized with dolomite percentages of over 80%. Dolomite content decreases in the deepest drilled sections to values below 10%. The sediments and rocks from Stock Island are dominated by low-Mg calcite in the upper zones and by increasing dolomite values in the deeper sections. Quartz content in the analyzed samples from the Stock Island core are throughout below 5%. In the deeper section of this site, dolomite seems to occur more patchy than in the Long Key core. Several samples below 209 m show almost pure dolomitization, while others are characterized by no significant dolomite content. Except four samples that have minor amounts of aragonite, all samples contain neither a detectable content of aragonite nor of high-Mg calcite, indicating that diagenetic reactions already dissolved or replaced these meta-stable minerals.

4.2. Wireline logs

A suite of wireline logs were available from both core holes. In this study, we mainly used the sonic log, since it complements the data collected in the laboratory and provides a continuous downhole record of velocity trends.

Fig. 7 shows the sonic logs of the Long Key and Stock Island core holes and compares them with

Table 1
Physical properties and lithological characteristics of analyzed samples

Sample No.	Depth (m)	Depositional lithology	Porosity (%)	V_p (m/s)	V_s (m/s)	Dry bulk density	X-ray weight-percentages				
							Arag	Qtz	LMC	HMC	Dol
<i>Long Key Core</i>											
L1	6.0	coral boundstone	41.3	4927	2391	1.57	0	0	100	0	0
L2	14.9	coral boundstone	24.7	5520	2780	2.04	0	0	100	0	0
L3	40.6	peloidal-skeletal pack-grainstone	23.8	4106	1822	2.06	0	10	90	6	0
L4	46.5	quartz-rich, skeletal wackestone	12.9	4945	2745	2.36	0	20	66	0	13
L35	49.2	quartz sand	52.0	2121	–	1.28	0	86	8	0	6
L34	84.7	quartz sand	45.0	1710	1142	1.47	0	87	13	0	0
L33	129.1	quartz sand	43.1	2156	1262	1.55	0	90	10	0	0
L32	143.9	quartz sand	46.2	2220	1250	1.45	0	71	29	0	0
L31	187.4	quartz sand	44.8	2208	–	1.46	0	93	3	0	4
L30	190.5	quartz sand	44.8	2234	–	1.47	0	87	9	0	4
L5	199.3	skeletal packstone	42.8	2721	1271	1.56	0	2	67	0	31
L6	209.6	skeletal packstone	41.6	2487	1200	1.59	0	0	72	0	28
L7	226.0	skeletal packstone	45.5	2718	1297	1.48	0	0	95	0	5
L8	236.1	skeletal pack-grainstone	37.7	2755	1298	1.69	0	1	93	0	6
L9	245.0	skeletal grain-packstone	30.8	3614	1976	1.88	0	1	97	0	2
L10	262.7	skeletal grainstone	44.0	2417	1090	1.55	0	1	57	0	43
L11	263.7	skeletal wackestone? (sucrosic dolomite)	42.1	2522	1288	1.62	0	1	12	0	87
L12	281.7	skeletal grain-packstone	46.0	2482	1185	1.46	0	0	71	0	29
L13	290.7	skeletal wackestone? (sucrosic dolomite)	39.1	2600	1176	1.69	0	0	13	0	87
L14	294.7	skeletal grainstone	48.4	2789	1362	1.44	0	0	18	0	82
L15	305.7	nothing preserved (sucrosic dolomite)	32.8	4016	2218	1.88	0	1	1	0	98
L16	309.6	red algae packstone? (mimetic dolomite)	14.3	5965	3253	2.44	0	0	13	0	87
L17	313.4	nothing preserved (sucrosic dolomite)	35.0	5076	2590	1.82	0	0	4	0	96
L18	314.5	skeletal grain-packstone	32.5	3102	1684	1.81	0	0	64	0	36
L19	316.1	skeletal grainstone	32.4	3430	1608	1.85	0	0	94	0	6
L20	318.5	red algae wackestone? (mimetic dolomite)	29.1	5021	2519	1.96	0	0	3	0	97
L21	325.8	skeletal wackestone? (sucrosic dolomite)	37.5	3187	1340	1.76	0	0	11	0	89
L22	326.2	red algae grainstone? (sucrosic dolomite)	29.1	5021	2519	1.96	0	0	5	0	95
L23	328.9	skeletal grainstone	35.6	3946	2041	1.74	0	0	92	0	8
L24	333.8	patchy, skeletal wacke-grainstone	30.9	4575	2348	1.88	0	0	98	0	2
L25	351.7	skeletal wackestone	49.1	2340	1203	1.39	19	0	62	0	19
L26	409.6	skeletal grainstone	46.7	2789	1500	1.44	0	2	98	0	0
L27	410.0	skeletal grainstone	51.4	2450	1216	1.31	0	0	95	0	5
L28	418.2	skeletal grainstone	46.7	2880	1431	1.45	0	2	98	0	0
L29	422.9	peloidal grainstone	35.8	2887	1485	1.75	0	0	100	0	0
<i>Stock Island Core</i>											
S1	21.54	coral boundstone	24.4	5555	2480	2.04	0	0	99	1	0
S2	40.06	skeletal pack-wackestone	38.4	4375	2258	1.67	0	1	99	0	0
S3	62.15	skeletal grainstone	46.1	2537	1138	1.46	0	2	98	0	0

Table 1 (continued)

Sample No.	Depth (m)	Depositional lithology	Porosity (%)	V_p (m/s)	V_s (m/s)	Dry bulk density	X-ray weight-percentages				
							Arag	Qtz	LMC	HMC	Dol
S4	72.52	skeletal pack-grainstone	32.8	4030	2290	1.81	0	3	97	0	0
S5	90.86	skeletal grain-packstone	48.2	2689	1238	1.40	0	4	90	0	6
S6	112.6	skeletal grain-packstone	52.7	2377	1190	1.27	0	5	88	0	7
S7	128.9	skeletal grainstone	55.8	2393	1232	1.21	0	3	90	0	7
S8	142.1	skeletal grain-packstone	54.8	2481	1112	1.23	0	2	82	0	16
S9	158.1	skeletal grain-packstone	53.4	2312	1262	1.29	0	5	68	0	27
S10	182.1	skeletal grain-packstone	54.5	2439	1109	1.24	0	1	86	0	13
S11	194.5	peloidal-skeletal grainstone	54.1	2425	1270	1.26	0	2	90	0	8
S12	200.0	skeletal grainstone	52.7	1878	1132	1.31	0	2	86	0	12
S13	206.5	peloidal-skeletal grainstone	50.8	2509	973	1.37	0	3	70	0	27
S14	209.9	grainstone? (mimetic dolomitization)	22.2	5435	2825	2.17	3	0	20	0	78
S15	215.1	skeletal pack-grainstone	8.7	5912	3287	2.58	0	0	11	0	89
S16	234.0	nothing preserved (sucrosic dolomite)	17.2	5263	2986	2.35	0	0	0	0	100
S17	251.9	echinoderm grainstone	50.5	2698	1253	1.35	0	0	97	0	3
S18	264.1	peloidal-skeletal grainstone	41.2	3062	1612	1.62	9	0	87	4	0
S19	305.4	skeletal grainstone	23.5	4449	2321	2.06	6	2	91	1	0
S20	320.6	foraminiferal wackestone	27.9	4837	2762	2.05	0	1	6	0	93

Arag=aragonite, Qts=quartz, LMC=low-Mg calcite, HMC=high-Mg calcite, Dol=dolomite.

the velocity data from discrete miniplugs used in the laboratory analyses. Despite different methods of measuring velocity with different resolution and different frequencies (1 MHz for the laboratory; 1–100 kHz for the sonic log) the two datasets match well and most miniplug velocities clearly coincide with the trends seen in the sonic logs. Only the section of fine-grained carbonates in the Stock Island Formation shows a systematic offset between log and miniplug data. In this zone, laboratory velocities are always approximately 400 m/s higher than log velocities (Fig. 7). This is most likely caused by the high-porosity/low-velocity lithology of these fine-grained carbonates that tend to consolidate and compact intensely under pressure. The chosen effective pressure of 8 MPa, at which the plug data are taken, is in fact higher than the effective pressure of the in situ sediments in that section (approximately 4 MPa). The effect of this difference in effective pressure can be seen on Fig. 5 and explains the observed systematic offset between the two types of velocity in highly porous zones.

5. Discussion

5.1. Controls on velocity

Velocity is a complex product of several parameters which together control range and absolute values of velocity in the buried sedimentary rocks. In the next sections we discuss the controlling factors and compare their significance in controlling the acoustic properties.

5.1.1. Effective pressure

In general, the sonic velocities increase with increasing effective pressures (Fig. 5). At high confining pressures, V_p and V_s are usually faster than at low pressures. Samples with a low velocity show a much stronger increase in velocities with increasing effective pressures, whereas samples with an already high velocity at low effective pressure increase velocities only slightly. The intensity of the increase is mainly caused by closing of microcracks, compaction, and consolidation of the rock fabric, which is stronger in high-porosity samples.

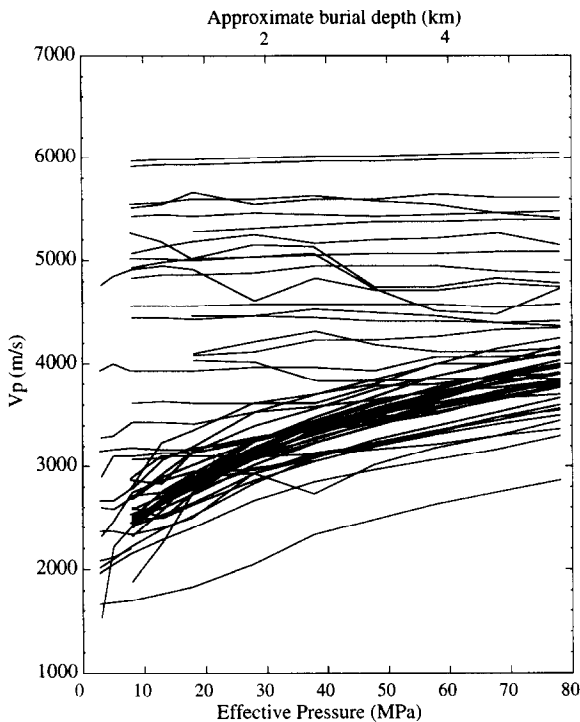


Fig. 5. Velocity as a function of pressure. Lines represent velocities of discrete samples at increasing effective pressures. Conversion to burial depth (upper x-axis) based on a rock density of 2.5 g/cm³ and on a fluid density of 1.0 g/cm³. Some samples show decreasing velocities at increasing pressures, indicating fabric destruction in the pressure vessel due to collapse and fracturing.

Some samples show, however, decreasing velocities at increasing effective pressures, which indicates cracking and disintegration of friable frame-forming textures at elevated pressures. The strong pressure dependence of velocities in highly porous rocks explains the offset of V_p values from miniplug data and from the sonic log in homogenous low-velocity zones (Fig. 5).

5.1.2. Burial depth

The downhole trends of velocity can be recognized in both, log and miniplug data (Fig. 7). There is no simple correlation between depth and velocity. Velocity inversions can be recognized throughout the cores. This lack of correlation is enigmatic, if one only considers the positive correlation between effective pressure and velocity (Fig. 5), but can be explained by selective diagen-

esis. Diagenesis is highly variable between stratigraphic layers, cementing some layers while others are less cemented or even partially undergo dissolution. Consequently, in a vertical section, highly cemented horizons that yield fast velocities may alternate with porous, low-velocity intervals, depending on the diagenetic potential of the sediment. Thus, the effect of increased burial (increasing effective pressure) is totally overshadowed by diagenetic effects independent of burial depth. Consequently, burial depth alone has no significant impact on controlling acoustic properties of the studied sedimentary rocks.

5.1.3. Porosity and pore type

A plot of porosity versus velocity shows an expected general trend of decreasing velocities with increasing porosities (Fig. 8). The scattering, however, is considerable and, though porosity is the primary control on velocity, total porosity is not the only constraint on velocity. For example, at a porosity of 35%, the velocities range between 3000 and 5500 m/s. Therefore, there have to be some other rock properties that influence the sonic velocity, such as pore type, quartz content and dolomite content. Based on the results of another study (Anselmetti and Eberli, 1993), we consider that much of the scatter is due to the occurrence of different pore types that all have predictable effects on the elastic properties of a sediment. The different pore types that were classified based on thin-section observations are *interparticle*, *intraparticle*, *intercrystalline*, *moldic* and *intraframe* porosity (Choquette and Pray, 1970). Though microporosity is an important factor in total porosity, it could not be quantified by optical petrography and is not considered in this study. Fig. 9 plots velocity versus porosity with discrimination of pore types. This display indicates that the individual pore types cluster to a certain degree and cause part of the scattering. For example, all pore types that are embedded in a rigid rock framework (such as moldic or intraframe pores) account for most of the samples that have relatively high velocity at high porosities, thus plotting far above the average best-fit line through all samples (Fig. 9). In contrast to these high-velocity samples, samples with pores in between individual compo-

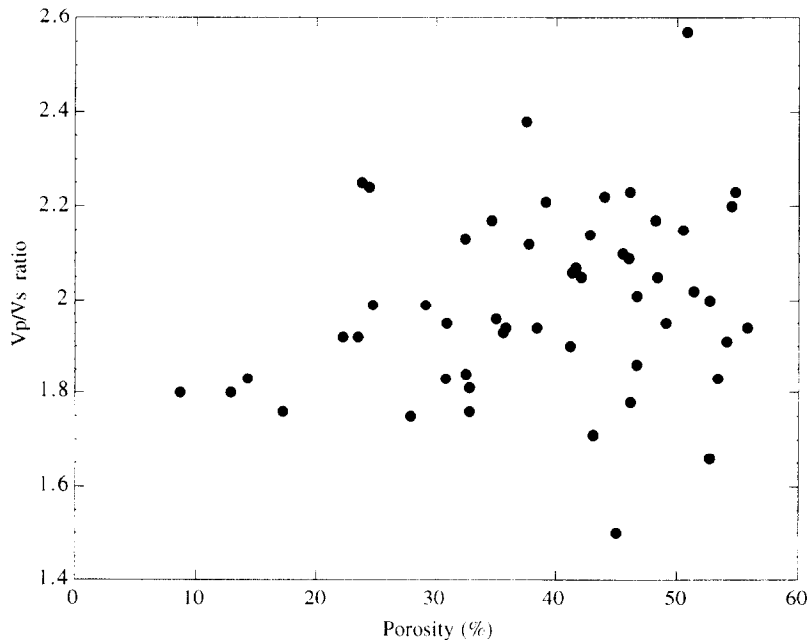


Fig. 6. V_p/V_s ratio as a function of total porosity. The V_p/V_s ratios have a wider range and higher values toward higher porosities, documenting the sensibility of V_s to fabric weakening.

nents (interparticle pores) mostly have very low velocities, because their fabric provides no frame that could enhance elastic properties, but they are composed of an accumulation of individual non-cemented grains that do not favor a fast transmission of the acoustic signal. In contrast to pure carbonates, however, in which total porosity and pore types together control most porosity–velocity variations (Anselmetti and Eberli, 1993), the petrophysical properties of these mixed siliciclastic sediments obviously are influenced by other parameters, such as quartz content (see below) or possibly pore or grain shape and orientation.

5.1.4. Quartz sand content

The cored lithologies are composed of varying percentages of quartz sand. In particular the Long Key Formation consists of almost pure quartz sand, whereas the time-equivalent Stock Island Formation contains an average of 5% quartz sand within a matrix of fine-grained limestones (Fig. 4).

A plot of velocity versus porosity and discrimination of percent quartz content documents that all samples of pure quartz sand form the lowest

velocity values at high porosities (Fig. 10). There are only two samples other than from the quartz sands of the Long Key Formation, which have a quartz content significantly higher than 5%. These samples are marked in the velocity–porosity cross-plot in Fig. 10, and they interestingly have lower velocities, relative to same porous pure carbonate samples. This relationship confirms the assumption, that quartz content has the effect of lowering velocities (Kenter et al., 1997). This relationship is not only caused by the lower crystal velocity of quartz, but indirectly also by the lower diagenetic potential of quartz grains. Compared to metastable carbonates, quartz at low burial depths is diagenetically inert and thus grain dissolution and reprecipitation, which could increase velocities, is inhibited. In addition, quartz grains do not provide a preferred substrate for calcite cements to grow on. As a consequence, increasing quartz content usually results in relatively low velocity. The whole quartz sand section of the Long Key Formation, however, has no significantly different log signature than the Stock Island Formation, which mainly consists of fine-grained carbonates (Figs. 3, 4 and 7).

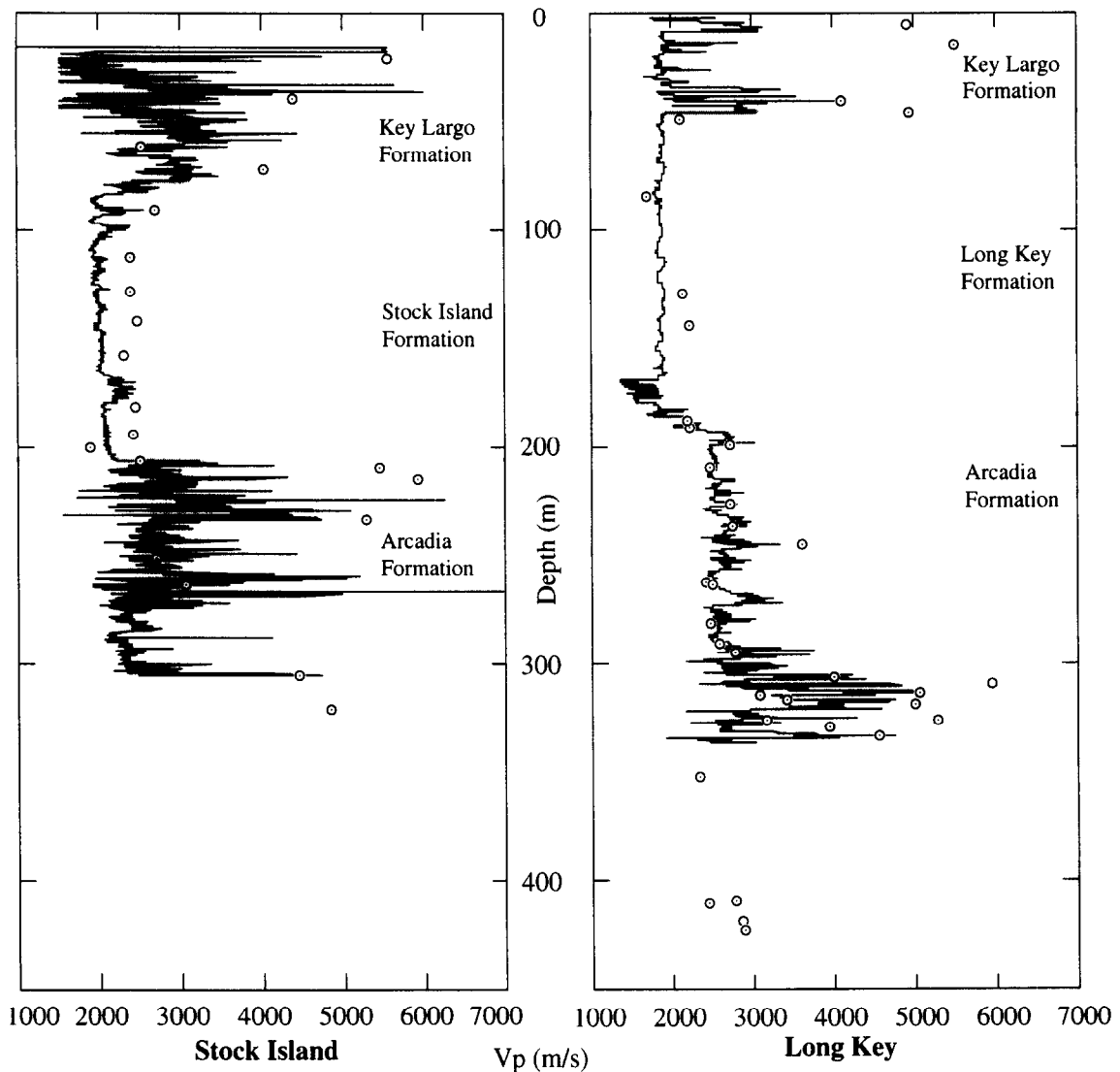


Fig. 7. Sonic logs of Long Key and Stock Island core holes compared with sonic velocity data measured on discrete samples in the laboratory. The differences between laboratory and log data are caused by different resolutions of the two techniques and, in the homogenous shallow sections, by higher effective pressure in the laboratory than under burial conditions (see text for explanation).

5.1.5. Dolomite content

Measurements from miniplugs show a wide variety of percentage of dolomite and types of dolomite. Two major types of dolomite can be recognized (Dawans and Swart, 1988), (1) micro-sucrosic dolomite consisting mainly of isolated rhombohedra floating in a carbonate matrix and (2) fabric-preserving, mimetic dolomite that has principally replaced precursor grainstones, preserv-

ing most of the original fabric with grains replaced and cement precipitated. If velocity is plotted against dolomite content (Fig. 11), no general correlation can be recognized and datapoints seem to scatter randomly, which is in agreement with results of Anselmetti and Eberli (1993). However, a plot of V_p versus porosity with discrimination of the percentage of dolomite shows clearly a trend of increasing V_p with increasing percentage of

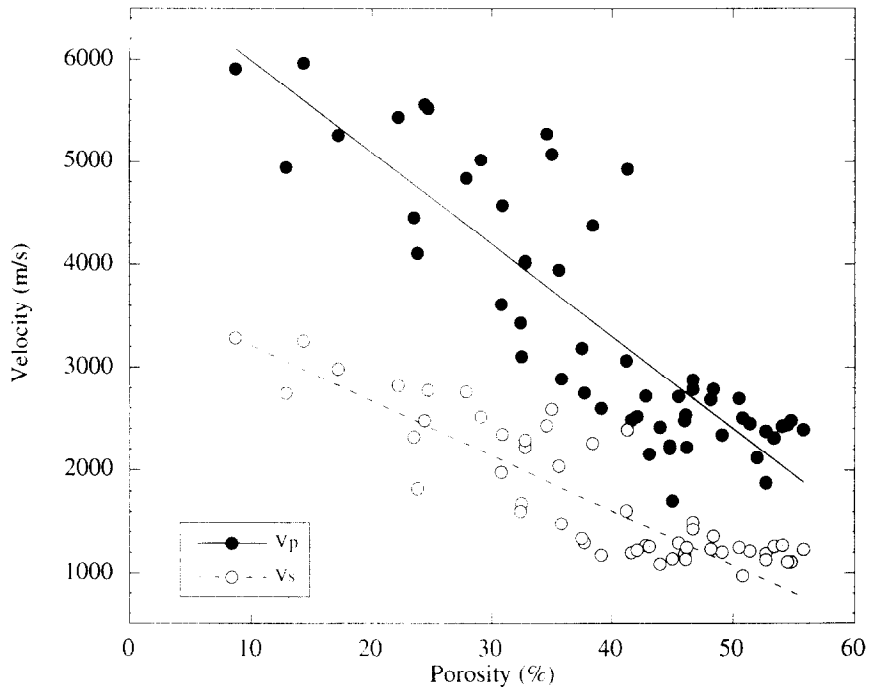


Fig. 8. Compressional (V_p) and shear-wave (V_s) velocity versus porosity with linear best-fit lines. Despite the inverse trend, both V_p and V_s display significant scatter for constant porosity. This scatter can partly be attributed to the occurrence of different principal pore types.

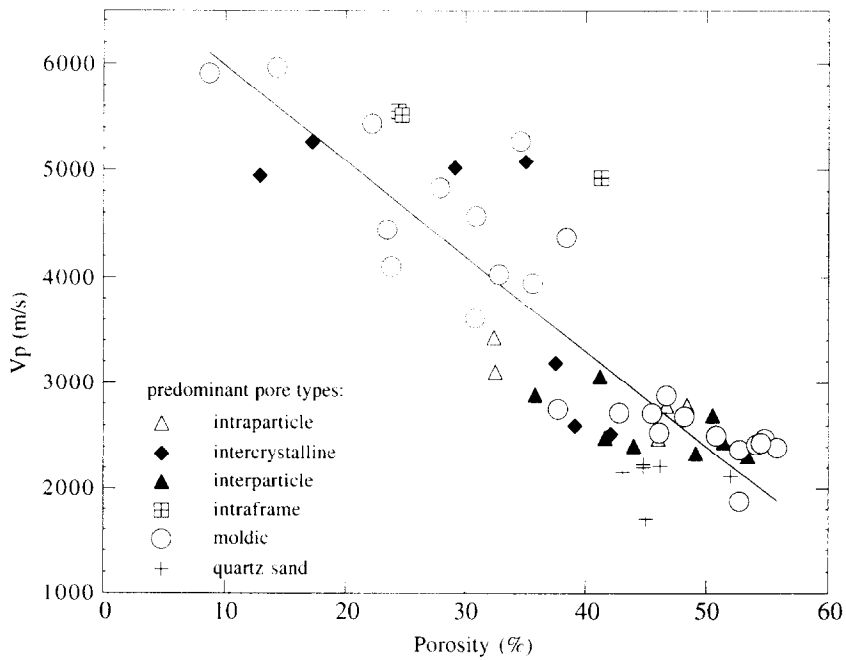


Fig. 9. V_p as a function of porosity. Principal pore types are indicated. Samples with frame-forming pore types cluster at higher velocities than samples characterized by intergranular porosity or samples with a high content of microporosity.

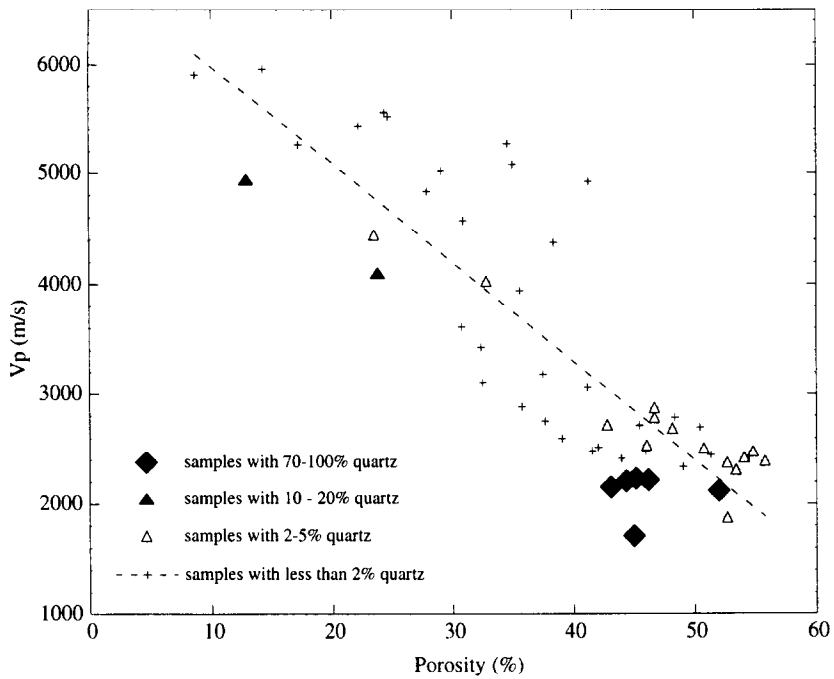


Fig. 10. Crossplot of V_p versus total porosity with percent quartz sand content indicated. A high content of quartz sand results in lower velocities than most carbonates, because quartz sand is resistant to dissolution and provides no preferred substrate for cements, which could enhance elastic properties of the sediment.

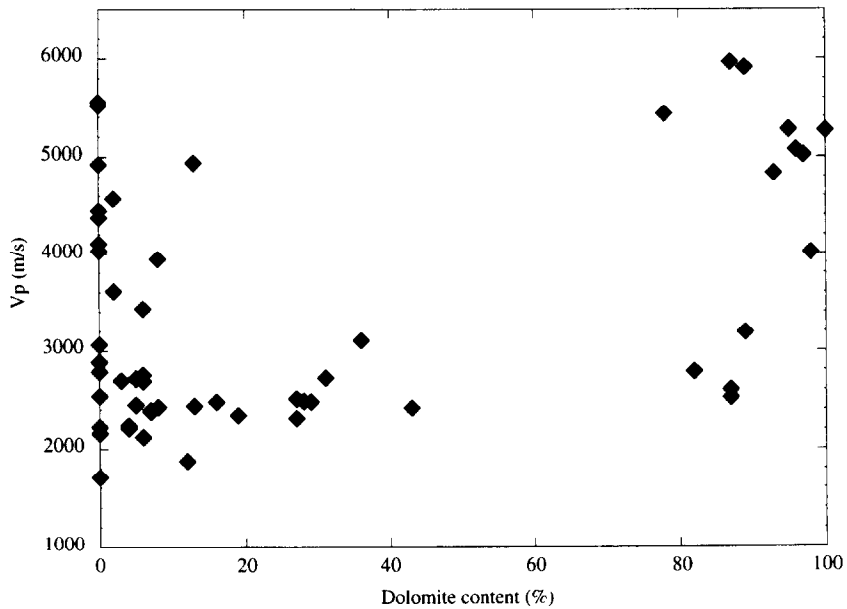


Fig. 11. Crossplot of dolomite content and V_p . Note the lack of correlation between these two parameters. Dolomite percentage alone is no proxy for velocity.

dolomite (Fig. 12). All highly dolomitized samples have higher V_p than the samples with lower percentages of dolomite, which implies that dolomitization increases elastic properties. Below a certain threshold porosity, which is in this study around 30% (Fig. 12), velocities of dolomite rocks seem to increase drastically. This relationship is also recognized for microsucrosic dolomites, usually believed to result in lower velocities (Anselmetti and Eberli, 1993). Although these dolomites form initially a loose aggregate with low elastic constants, the data shown in Fig. 12 indicate that increasing sucrosic dolomitization yields higher velocities as well. This might be explained with the observation of the threshold porosity, below which velocity increases. Evidently, the isolated rhombohedra grow together below this critical porosity and, as a consequence, form a connected frame-like fabric with higher elastic properties than unconnected dolomite crystals. The highest velocities of sucrosic dolomites, however, are still lower than the velocities of fabric-preserving dolomites, which usually result in the highest measured velocities (Fig. 12).

6. Implications for seismic reflection pattern

All the described variations of physical properties, in particular sonic velocity, have their effect on the seismic reflection pattern. Three approaches were conducted to obtain information on the seismic response of the cored sedimentary rocks: (1) establishing the petrophysical signatures, in particular the distribution of acoustic impedance, (2) calculation of synthetic seismograms of different polarities and frequencies in both core holes using impedance logs created from sonic and density logs, and (3) evaluation of the nearest available seismic section, which is compared with the cored lithologies and the synthetic seismograms.

6.1. Petrophysical signatures of prograding Stock Island and Long Key Formations

One of the most striking lithologic features encountered in the two core holes is the distinct lithologic difference between the time-equivalent

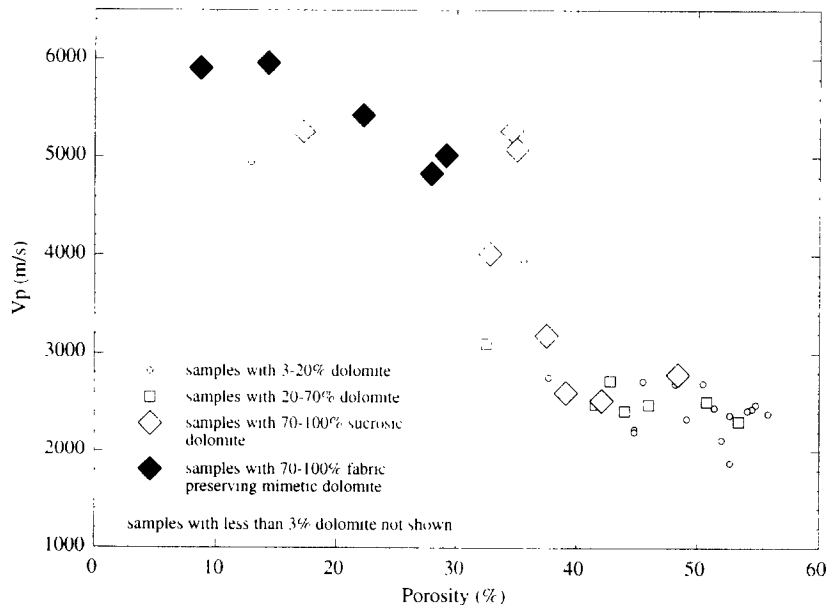


Fig. 12. V_p as a function of porosity with percentage of dolomite indicated. Note the trend of increasing velocities with increasing percentages of dolomite. A porosity of 30% seems to be a threshold value, below which V_p increases sharply. This threshold porosity might coincide with the dolomite rhombohedra growing together, yielding a framework with higher elastic properties.

Stock Island and Long Key Formations. The Long Key Formation consists of quartz sands while the Stock Island Formation consist of fine-grained deeper-water carbonates (Figs. 3 and 4). These two formations conceivably interfinger or they may show a gradual transition between the two core holes (Warzeski et al., 1996). Because the two core holes are located along the island chain of the Florida Keys, which are connected by a road using several bridges over shallow-water areas, neither marine nor land seismic techniques can be applied to directly seismically image this transition zone. The acquired grid of multichannel seismic data seaward of the Florida reef tract, however, connects the wider areas of each core hole with each other, yielding a seismic image of a possible transition between the two formations. The available cores provide an opportunity, to investigate the petrophysical signature of the two formations in order to investigate the seismic response of the sand and fine-grained carbonate lithologies. It will be shown, however, that despite the differences in lithology, both formations have the same petrophysical and, consequently, seismic signature, making predictions of lithology based on a seismic image extremely difficult.

In this study, six miniplugs were petrophysically analyzed from the Long Key Formation and eight miniplugs from the Stock Island Formation. The photomicrographs in Fig. 4 display the lithologic characteristics of each formation. The porosity–velocity values of the samples are plotted in Fig. 13a. Compared with all samples from both cores, the Stock Island and Long Key Formations have all very low and very uniform values. The homogeneous velocity distribution can be recognized in the sonic logs (Figs. 7 and 14), which display in both sites an equivalent section that lacks any significant scattering. The fine-grained limestones of the Stock Island Formation have porosities of 50–55% with V_p averaging 2200–2600 m/s while the quartz sand from the Long Key core is less porous (42–48%) but have lower V_p (2000–2300 m/s). The reason for this reverse correlation is that the carbonates are characterized by mainly moldic porosity, yielding higher velocities, while the quartz sands have lower matrix velocities and solely interparticle porosity, both of which

result in lower velocity, despite the lower porosity. These initial differences in velocity and porosity between the two formations, however, do not result in different acoustic impedance values. The recognized separate porosity–velocity clusters shown in Fig. 13a lie on the same line of equal acoustic impedance, calculated for densities of calcite (2.710 g/cm³) and quartz (2.648 g/cm³) respectively (Carmichael, 1989). The resulting impedance values are for both formations identical and amount to an average of 4.25×10^6 kg/s m² with very low scatter (Fig. 13b). Consequently, a possible interfingering of the two formations or a gradual transition between them is not expected to result in significant changes in acoustic impedance and thus should not yield a seismic reflection.

6.2. Synthetic seismograms

The values from the sonic log of both core holes were multiplied with values from the density logs in order to obtain an impedance log. This impedance log was converted into a spike section (reflection events) and convolved with several Ricker zerophase wavelets of variable frequencies between 20 and 100 Hz. Since the cores are not positioned directly on a seismic section, no checkshot calibration was available to fit the synthetic seismograms to the seismic data. The resulting synthetic seismograms are plotted in time with positive and negative polarity to show the influence of chosen polarity (Fig. 14). All seismograms can be compared with the sonic logs (Figs. 7 and 14) that are displayed in depth.

The effects of the distribution of petrophysical properties mentioned above are clearly recorded by the calculated synthetic seismograms. The seismic pattern of the displayed seismograms can be subdivided into a high-amplitude seismic facies at the top and at the bottom, and a zone with low amplitudes or seismic transparency between. Comparison with the sonic log shows that this transparent to low-reflectivity zone originates from the very homogeneous, low-velocity signature in the Stock Island and Long Key Formations, whereas the high amplitudes are caused by the petrophysically highly variable shallow-marine carbonates of the underlying Arcadia Formation

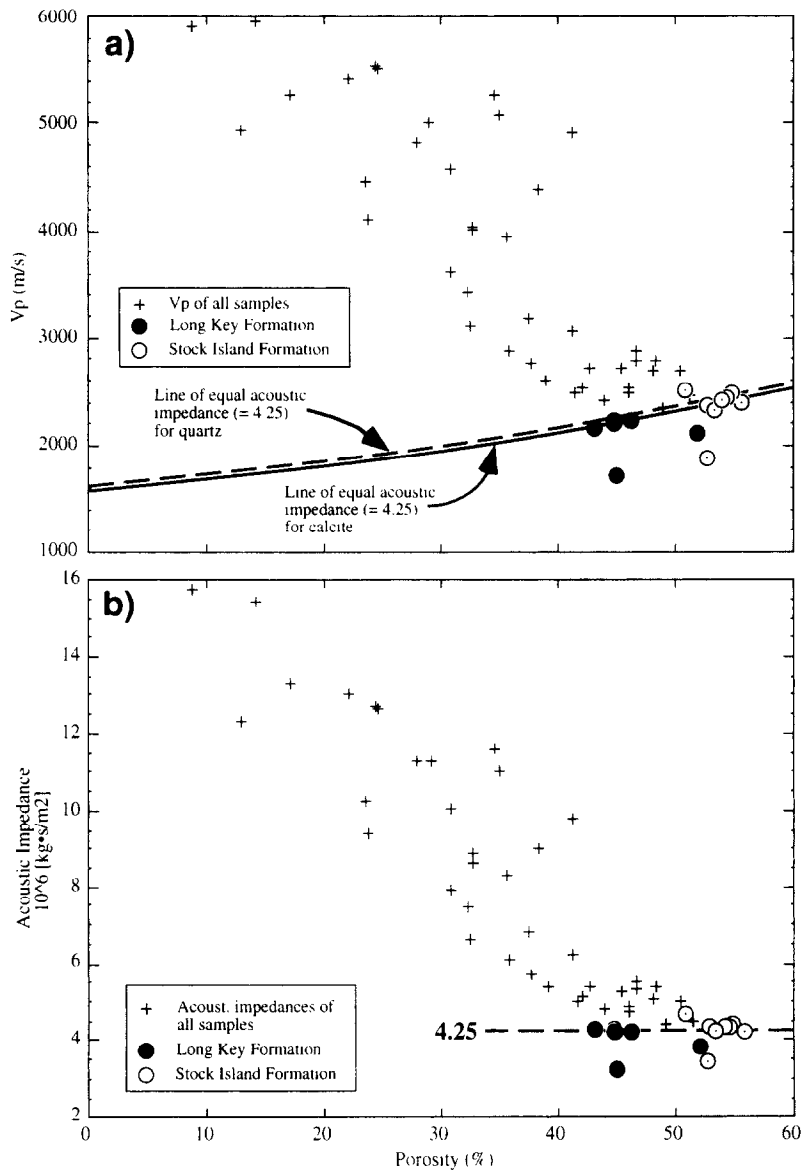


Fig. 13. Petrophysical signatures of Long Key and Stock Island Formations: (a) Porosity- V_p diagram, showing by two separate data clusters the Long Key and Stock Island Formations, based on porosity and velocity differences. Both data clusters lie on the same constant impedance value line (4.25×10^6 kg/s m²) for calcite and quartz densities, respectively. (b) Acoustic impedance versus porosity diagram indicating that initial velocity differences do not result in impedance differences. Together, velocity and bulk densities reversely equalize the observed velocity/porosity differences, resulting in identical impedances.

and the overlying Key Largo and Miami Limestones (Figs. 2 and 3). This distribution pattern of seismic facies is independent of chosen frequency or polarity. An increase in frequency only increases resolution and thus the numbers of

reflection events, while a shift in polarity can shift the location of a prominent reflection event by accentuating the reverse part of the reflection wiggle. An intriguing observation is that these two lithologically different prograding units (Stock

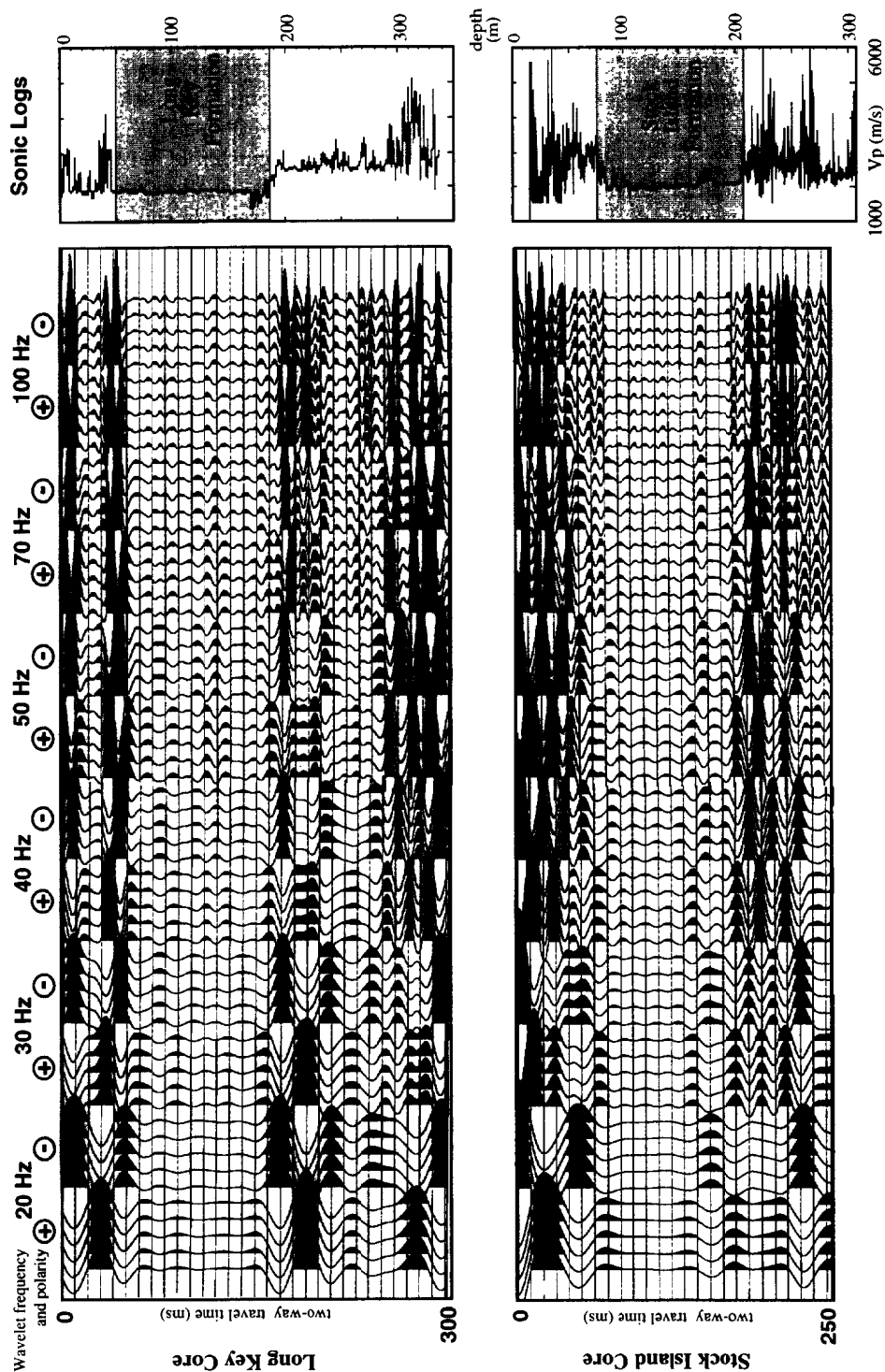


Fig. 14. Synthetic seismograms of the Stock Island and Long Key core holes. Seismograms were calculated using sonic and density logs. The reflection events were convolved with Ricker zero-phase wavelets with frequencies ranging from 20 to 100 Hz and displayed as both positive and negative polarity. The sonic logs of both core holes are displayed at the right-hand side. The correlation between the displays of log and seismic traces is only visually matched. True travel time-to-depth correlation is not linear and depends on formation velocities. Note the seismically transparent Long Key and Stock Island Formations, compared to the high-reflective shallow-water carbonates above and below (Key Largo and Arcadia Formations).

Island and Long Key Formations) have similar synthetic seismic patterns, a result of the similar impedance signatures.

6.3. Correlation with nearby multichannel seismic data

A grid of high-resolution multichannel and single channel data is available consisting of lines running parallel to the island approximately 10 km offshore in deeper water, and of few lines perpendicular to the Keys that reach within 2 km to the cores into shallower water (Fig. 1). The seismic lines close to the cores are, however, not useful, because the high velocity contrast of the Holocene–Pleistocene transition and the shallow depth cause shallow multiples and intense ringing on these seismic data. In contrast, the deeper-water seismic sections from 15 km offshore image the southeast continuation of the lithologic formations seen in the cores. The seismic data located offshore between the projected positions of Stock Island and Long Key (Figs. 1 and 15), display a seismically low-reflective to transparent zone that is very similar to the synthetic data. This zone most likely images the seaward continuation of fine-grained limestones or quartz sandstones (Warzeski et al., 1996). They form a low-reflective, chaotic unit that is characterized by lower reflection amplitudes and seismic transparency, which contrast to the high-amplitude and continuous reflections from the overlying and underlying shallow-marine deposits (Fig. 15). Both contacts to the over- and underlying shallow-water carbonates are sharp and irregular, displaying frequent incisions cutting into the lower units and yielding typical cut-and-fill geometries.

The similarity to the synthetic seismic patterns and the correct stratigraphic position make it very likely, that the lithology of the reflection-free zone is either the petrophysically very homogenous quartz sand of the Long Key Formation or the fine-grained carbonates of the Stock Island Formation. The identical petrophysical signatures of the two lithologies, as described above, do not allow for further identification of the lithologies. One cannot predict whether the imaged section represents a quartz sand or a fine-grained carbon-

ate lithofacies, or even a mixture or interfingering of these two endmember lithologies. The distances from the imaged section (Fig. 15) to the two drillsites is similar for both sites (Fig. 1), so that geographical arguments can not discern those facies neither. The whole seismic sequence, however, is clearly distinguishable between the overlying and underlying shallow-water carbonate sequences which contrast sharply with their high-reflective, coherent seismic facies.

All these observations of the seismic reflection pattern imply that, in this case, the marine seismic sections can neither be used to distinguish between prograding pure quartz sand and fine-grained limestone, nor can the seismic data image a possible facies transition or an intercalation between them. Both the impedance homogeneity but also the absolute impedance pattern are extremely similar and probably yield the same seismic response, which, based on the tremendous differences in lithologies (Fig. 4), is rather surprising. The only option to distinguish on seismic data between the two lithologies is to obtain more information of geometries of these prograding formations. The two lithologies might be characterized by different angles of repose resulting in different clinoform angles or different stacking patterns, because siliciclastics tend to have lower slope angles than carbonates (Kenter, 1990). These additional characteristics could be resolvable on seismic data and might provide a tool to predict the lithofacies distribution in these prograding shelf deposits.

7. Summary and conclusions

Sonic velocity in the two cored sections is mainly controlled by three factors.

(1) Porosity and pore types have a major control on V_p and V_s . Total porosity alone, however, does not sufficiently determine velocity. In addition, the geometrical distribution of pores and solid phase is important for the velocity. Porosity occurring in a rigid rock framework results in higher elastic moduli and thus higher velocities than interparticle porosity.

(2) In general, an increase in percentage of dolomite results in an increase in velocity. Fabric-

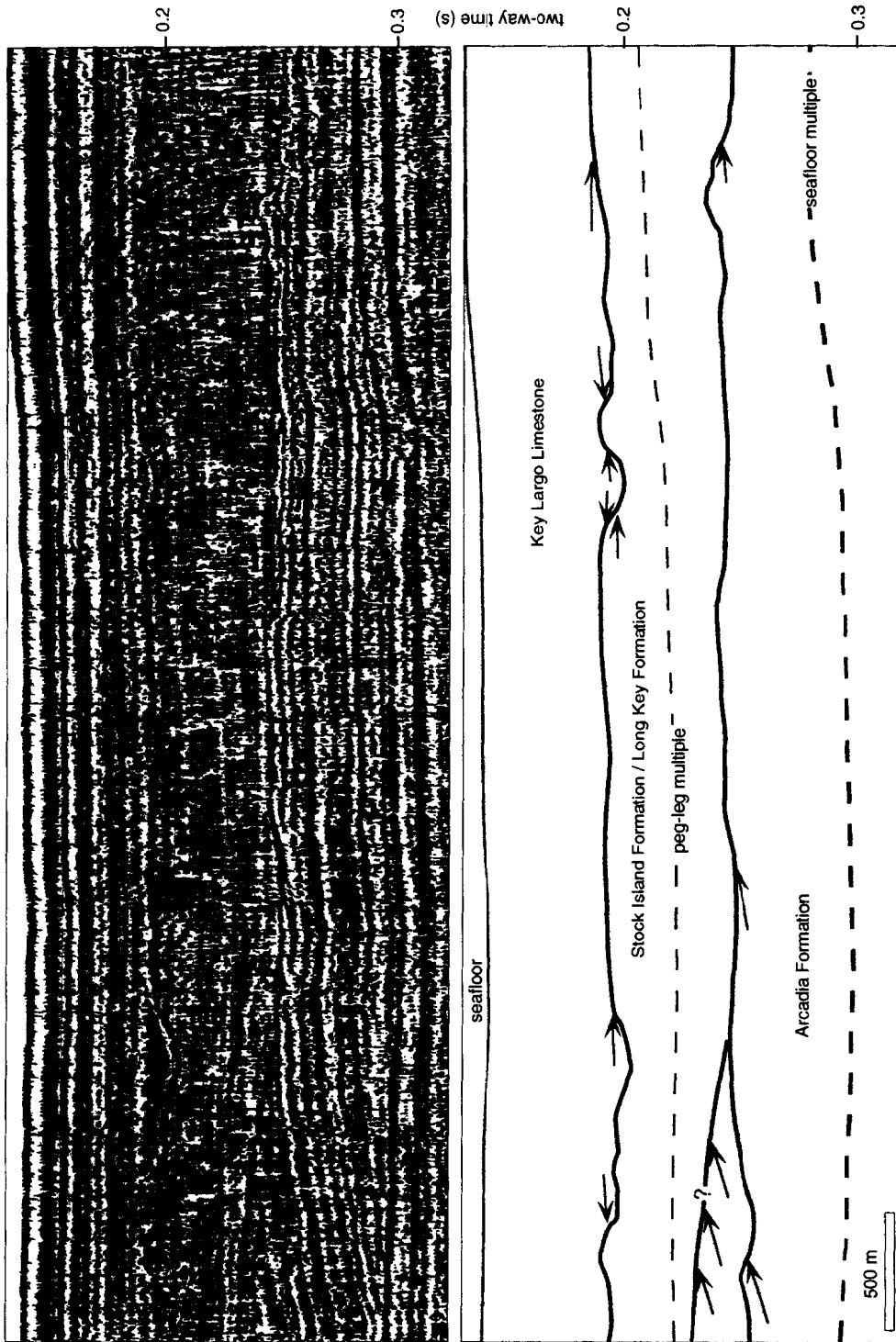


Fig. 15. Uninterpreted and interpreted seismic section located approximately 10 km offshore from Stock Island and Long Key core holes (for location see Fig. 1). Note the reflection free zone in between overlying and underlying units with high-amplitude reflections. The highly reflective zones are shallow-water carbonates of Key Largo Formation (above) and Arcadia Formation (below), while the transparent zone in between is the equivalent mixture or interfingering of the Stock Island and Long Key formations. Due to the similar petrophysical properties and the resulting almost identical seismic response, no further distinction can be made based only on the seismic reflection pattern. The observed seismic facies coincide with the synthetic seismograms shown in Fig. 14. Polarity of plotted sections is positive.

preserving mimetic dolomites yield highest velocities, whereas carbonates with sucrosic dolomitization only have high velocities with porosities under 30%. This porosity value might be indicative of a threshold porosity below which the individual dolomite rhombohedra become connected and form a crystalline framework with high velocities.

(3) A high quartz content results in lower velocities, because quartz is resistant to moldic grain dissolution. The chemical stability of quartz yields a low diagenetic potential in quartz-rich rocks. In contrast, unstable carbonate minerals are very sensitive to diagenetic alterations and can be quickly dissolved, cemented, undergo recrystallization or they can become replaced by dolomite, all of which can enhance the elastic properties of the rock.

Despite the differences in velocity, porosity, and mineralogy values, the resulting acoustic impedance values are identical for fine-grained, deeper-water carbonates (Stock Island Formation) and for quartz sands (Long Key Formation). The similarity in petrophysical signature in both formations causes a very similar seismic response, which makes gradual transitions or intercalations of the two lithologies seismically undetectable. This observation is confirmed on synthetic seismograms calculated from sonic and density logs of the two core holes and on nearby seismic sections, which both image the prograding deeper-water sediments with a low-reflective to transparent seismic facies, whereas all shallow-water carbonates are characterized by a highly reflective seismic image. As a consequence, seismic sections can not be used to distinguish between the prograding quartz sands of the Long Key Formation and the prograding fine-grained carbonates of the Stock Island Formation. This has to be taken into account when making interpretations from seismic images.

Acknowledgements

We would like to thank the Florida Geological Survey for the core borings, especially T.M. Scott and K.M. Campbell. The Aqueduct Authority granted access to the core sites. Density wireline logs were provided by the South Florida Water

Management District. The seismic profiles were acquired onboard R/V *Lone Star* operated by Rice University, Houston. We thank John Anderson, Dave Mucciarone, and the *Lone Star* crew for their efforts. Acquisition of the seismic lines was funded by the Industrial Associates of the Comparative Sedimentology Laboratory at the University of Miami. The synthetic seismograms were calculated in the seismic laboratory of the Geophysical Institute at the Swiss Federal Institute of Technology in Zürich. Financial aid from the Industrial Associates of the Comparative Sedimentology Laboratory is gratefully acknowledged. We thank Alan Buck for assistance in core preparations. We gratefully acknowledge the helpful reviews of Jeroen Kenter and Amos Nur.

References

- Anselmetti, F.S., Eberli, G.P., 1993. Controls on sonic velocity in carbonates. *Pure Appl. Geophys.* 141 (2-4), 287–323.
- Birch, F., 1960. The velocity of compressional waves in rocks to 10 kilobars. Part 1. *J. Geophys. Res.* 65, 1083–1102.
- Brewster-Wingard, G.L., Scott, T.M., Edwards, L.E., Weedman, S.D., Simmons, K.R., 1997. Reinterpretation of the peninsular Florida Oligocene: an integrated stratigraphic approach. *Sediment. Geol.* 108, 207–228.
- Brooks, G.R., Holmes, C.W., 1989. Recent carbonate slope sediments and sedimentary processes bordering a non-rimmed platform: Southwest Florida continental margin. In: Crevello, P.D., Wilson, J.L., Sarg, J.F., Read, J.F. (Eds.), *Controls on Carbonate Platform and Basin Development*. SEPM Spec. Publ. 44, 259–272.
- Carmichael, R.S. (Ed.), 1989. *Practical Handbook of Physical Properties of Rocks and Minerals*. CRC, Boca Raton, FL., 741 pp.
- Choquette, P.W., Pray, L.C., 1970. Geologic nomenclature and classification of porosity in sedimentary carbonates. *AAPG Bull.* 54, 207–250.
- Christensen, N.I., Szymanski, D.L., 1991. Seismic properties and the origin of reflectivity from a classic Paleozoic sedimentary sequence, Valley and Ridge province, southern Appalachians. *Geol. Soc. Am. Bull.* 103, 277–289.
- Cunningham, K.J., Ginsburg, R.N., Warzeski, E.R., Eberli, G.P., Guertin, L.A., 1995. Burial of a drowned carbonate platform by Pliocene siliciclastic in the Florida Keys (abstr.). *Geol. Soc. Am., Abstr. Progr.* 27, A-82.
- Cunningham, K.J., McNeill, D.F., Guertin, L.A., Scott, T.M., Ciesielski, P.F., de Verteuil, L., 1997. A new Tertiary stratigraphy for the Florida Keys and southern peninsula of Florida. *Bull. Geol. Soc. Am.*, in press.
- Dawans, J.M., Swart, P.K., 1988. Textural and geochemical

- alterations in late Cenozoic Bahamian dolomites. *Sedimentology* 35, 385–403.
- Dunham, R.J., 1962. Classification of carbonate rocks according to texture. In: Ham, W.E. (Ed.), *Classification of Carbonate Rocks*, A Symposium. AAPG Mem. 1, 108–121.
- Ginsburg, R.N., Brown, K.M., Chung, G.S., 1989. Siliciclastic foundations of South Florida's Quaternary carbonates (abstract). *Geol. Soc. Am., Abstr. Progr.* 21, A-290.
- Ginsburg, R.N., Cunningham, K.J., 1996. Siliciclastic foundation of South Florida Quaternary carbonates (abstract). 8th Annual Int. Coral Reef Symp., June 24–29, Panama City, Panama, p. 71.
- Guertin, L.A., McNeill, D.F., Lidz, B.H., Cunningham, K.J., submitted. Biochronology of the new Long Key Formation: Late Neogene siliciclastic foundation of the Florida Keys. *Mar. Micropaleontol.*
- Hamilton, E.L., 1980. Geoacoustic modeling of the sea-floor. *J. Acoust. Soc. Am.* 68, 1313–1340.
- Han, D., Nur, A., Morgan, D., 1986. Effects of porosity and clay content on wave velocities in sandstones. *Geophysics* 51 (11), 2093–2107.
- Jordan, G.F., Malloy, R.J., Kofoed, J.W., 1964. Bathymetry and geology of the Pourtales Terrace, Florida. *Mar. Geol.* 1, 259–287.
- Kenter, J.A.M., 1990. Carbonate platform flanks: slope angle and sediment fabric. *Sedimentology* 37(5), 777–794.
- Kenter, J.A.M., Podladchikov, F.F., Reinders, M., Van der Gaast, S.J., Fouke, B.W., Sonnenfeld, M.D., 1997. Parameters controlling sonic velocities in a mixed carbonate-siliciclastics Permian shelf-margin (upper San Andres formation Last Chance Canyon, New Mexico). *Geophysics* 62, 1–16.
- Locker, S.D., Hine, A.C., 1995. Late Quaternary sequence stratigraphy, South Florida Margin. *Offshore Technol. Conf. OTC 7674*, pp. 319–327.
- Marion, D., Nur, A., Yin, H., Han, D., 1992. Compressional velocity and porosity in sand-clay mixtures. *Geophysics* 57, 554–563.
- Matson, G.C., Sanford, S., 1913. *Geology and ground waters of Florida*. U.S. Geol. Surv. Water Supply Pap. 41, 445 pp.
- Rafavich, F., Kendall, C.H.S.C., Todd, T.P., 1984. The relationship between acoustic properties and the petrographic character of carbonate rocks. *Geophysics* 49, 1622–1636.
- Vaughan, T.W., 1910. A contribution to the geologic history of the Florida Plateau. In: *Papers from the Tortugas Laboratory IV*. Carnegie Inst. Wash. Spec. Publ. 133, 99–185.
- Vernik, L., Nur, A., 1992. Petrophysical classification of siliciclastics for lithology and porosity prediction from seismic velocities. *AAPG Bull.* 76, 1295–1309.
- Vernik, L., 1994. Predicting lithology and transport properties from acoustic velocities based on petrophysical classification of siliciclastics. *Geophysics* 59, 420–427.
- Wang, Z., Hirsche, W.K., Sedgwick, G., 1991. Seismic velocities in carbonate rocks. *J. Can. Pet. Technol.* 30, 112–122.
- Warzeski, E.R., Cunningham, K.J., Ginsburg, R.N., Anderson, J.B., Ding, Z.-D., 1996. A Neogene mixed siliciclastic and carbonate foundation for the Quaternary carbonate shelf, Florida Keys. *J. Sediment. Res.* 66, 788–800.